

An efficient method for the calculation of quantum mechanics/molecular mechanics free energies

Christopher J. Woods, Frederick R. Manby, and Adrian J. Mulholland^{a)}

Centre for Computational Chemistry, School of Chemistry, University of Bristol, Bristol BS8 1TS, United Kingdom

(Received 6 August 2007; accepted 11 October 2007; published online 7 January 2008)

The combination of quantum mechanics (QM) with molecular mechanics (MM) offers a route to improved accuracy in the study of biological systems, and there is now significant research effort being spent to develop QM/MM methods that can be applied to the calculation of relative free energies. Currently, the computational expense of the QM part of the calculation means that there is no single method that achieves both efficiency and rigor; either the QM/MM free energy method is rigorous and computationally expensive, or the method introduces efficiency-led assumptions that can lead to errors in the result, or a lack of generality of application. In this paper we demonstrate a combined approach to form a single, efficient, and, in principle, exact QM/MM free energy method. We demonstrate the application of this method by using it to explore the difference in hydration of water and methane. We demonstrate that it is possible to calculate highly converged QM/MM relative free energies at the MP2/aug-cc-pVDZ/OPLS level within just two days of computation, using commodity processors, and show how the method allows consistent, high-quality sampling of complex solvent configurational change, both when perturbing hydrophilic water into hydrophobic methane, and also when moving from a MM Hamiltonian to a QM/MM Hamiltonian. The results demonstrate the validity and power of this methodology, and raise important questions regarding the compatibility of MM and QM/MM forcefields, and offer a potential route to improved compatibility. © 2008 American Institute of Physics. [DOI: 10.1063/1.2805379]

I. INTRODUCTION

Computer simulations that combine quantum mechanics (QM) with molecular mechanics (MM) are becoming increasingly important in the study of biological systems. QM/MM simulations have been found to be particularly useful for computational enzymology¹⁻⁷ and are now beginning to find use in docking,^{8,9} scoring,¹⁰⁻¹² and free energy calculations.¹³⁻²⁴ The potential advantages of using quantum mechanics to model part of the system are obvious: the improved physical description can better represent important physical phenomena, such as polarization, charge transfer, and bond breaking and formation. However, the disadvantage of QM/MM is that the computational expense of QM calculations is significantly greater than that of the MM calculation, and therefore QM/MM simulations are computationally demanding. This is a particular problem when QM/MM models are used during free energy calculations, as the high computational expense of the QM part of the calculation prevents the generation of the large ensembles of structures necessary to fully converge free energy averages. Current applications of QM/MM within free energy calculations¹³⁻²⁴ use a variety of methods to overcome this problem. Highly promising are methods¹⁷⁻²⁴ that involve the use of fast and approximate Hamiltonians to sample phase space, with the full QM/MM Hamiltonian being used sparingly to calculate or estimate free energies using only a lim-

ited subset of the generated configurations. Two main classes of methods will be discussed in this paper: (i) methods that use the fast Hamiltonian to estimate the relative free energy, and then use efficient algorithms to approximate the difference in free energy between the QM/MM and fast Hamiltonian, and (ii) methods that use the fast Hamiltonian as a means of enhancing sampling of the QM/MM Hamiltonian, thereby producing ensembles correct for the QM/MM Hamiltonian that can be fed directly into free energy methods such as free energy perturbation (FEP).

The first class of methods, typified by the approach developed Warshel and co-workers^{17,18} uses the free energy cycle shown in Fig. 1. First, the free energy change is estimated using an approximate, reference Hamiltonian (e.g., either a pure MM Hamiltonian^{19-21,25} or an empirical valence bond potential^{17,18}). This estimate is then corrected by calcu-

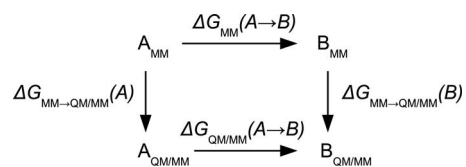


FIG. 1. The free energy cycle (Ref. 17 and 18) used to calculate the QM/MM free energy difference between systems A and B, $\Delta G_{QM/MM}(A \rightarrow B)$. The free energy difference between A and B is first estimated using an approximate potential (e.g., MM potential), giving $\Delta G_{MM}(A \rightarrow B)$. This is then corrected to the QM/MM value by calculating the free energy necessary to perturb system A from MM to QM/MM [$\Delta G_{MM \rightarrow QM/MM}(A)$] and the free energy to perturb system B from MM to QM/MM [$\Delta G_{MM \rightarrow QM/MM}(B)$].

^{a)}Electronic mail: adrian.mulholland@bristol.ac.uk

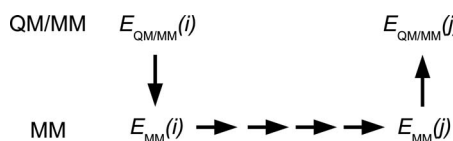


FIG. 2. Application of the Metropolis-Hastings (Ref. 27) algorithm to accelerate sampling of a system represented using a QM/MM Hamiltonian (Refs. 23 and 24). The Monte Carlo move starts at configuration i . The energy of this configuration is evaluated using the target QM/MM Hamiltonian [giving $E_{\text{QM/MM}}(i)$] and on an approximate (MM) Hamiltonian [giving $E_{\text{MM}}(i)$]. Standard Metropolis Monte Carlo moves are then attempted from configuration i using only the approximate MM Hamiltonian, until after a set number of moves, the system is in configuration j . The energy of configuration j is evaluated using both the QM/MM and MM Hamiltonians [giving $E_{\text{QM/MM}}(j)$ and $E_{\text{MM}}(j)$]. Configuration j is then accepted into the QM/MM ensemble according to the probability $\min\{1, \exp(-\Delta\Delta E/k_B T)\}$, where $\Delta\Delta E = [E_{\text{QM/MM}}(j) - E_{\text{MM}}(j)] - [E_{\text{QM/MM}}(i) - E_{\text{MM}}(i)]$.

lating the free energies necessary to change from the approximate Hamiltonian to the QM/MM Hamiltonian. In theory, this method will return the exact QM/MM free energy change. However, for the sake of efficiency, all of the sampling is performed using only the reference Hamiltonian, and the free energy difference between the reference and QM/MM Hamiltonians is calculated from a single-step FEP perturbation from the ensemble generated at the reference state. While this will converge well if there is good overlap between the phase space of the reference and QM/MM potentials, in practice the free energy may often not converge owing to the large fluctuations of the difference between the reference potential and the QM/MM potential.²¹ The focus of further development of this method is therefore the derivation of approximate reference Hamiltonians that are a good match to the target QM/MM Hamiltonian,¹⁸ and the use of the linear response approximation^{2,18,26} that improves convergence by running on both the approximate reference Hamiltonian and on the QM/MM Hamiltonian.

The second class of methods involves the use of an approximate Hamiltonian to speedup the sampling of phase space described by a QM²² or QM/MM^{23,24} Hamiltonian. These methods produce ensembles that are correct for the QM or QM/MM Hamiltonians used, and these ensembles can be used directly with free energy methods such as FEP. These methods work by using Monte Carlo sampling with a Metropolis-Hastings algorithm²⁷ (see Fig. 2). The algorithm works by using an approximate Hamiltonian (e.g., MM) to guide the Monte Carlo sampling of the QM or QM/MM Hamiltonian. The advantage is that the majority of the Monte Carlo moves require evaluations using only the approximate Hamiltonian, yet the form of the Monte Carlo acceptance test means that an ensemble that is rigorously correct for the QM or QM/MM Hamiltonian is sampled. The method was popularized for application to Monte Carlo sampling of QM and QM/MM Hamiltonians by Iftimie *et al.*,^{22,23} who coined the name “molecular mechanics based importance function” (MMBIF). The Metropolis-Hastings algorithm is generally applicable and can be applied to any situation where an expensive-to-evaluate potential can be approximated by a cheap potential. The power of this algorithm continues to be rediscovered,^{28,29} and it has been applied to accelerate Monte Carlo sampling of implicit solvent force fields³⁰ and the Ewald sum for long range electrostatics.³¹

One of the problems with the MMBIF method is that its efficiency depends on the level of phase-space overlap between the QM/MM and MM Hamiltonians. If the overlap is poor, then the probability of accepting each Metropolis-Hastings Monte Carlo move will be low, and convergence of the free energy averages will be poor. This is a similar problem to that encountered in the first class of methods, where if the overlap is poor, the estimate of the difference in free energy between the QM/MM and MM potentials will fail to converge. As in the case of the first class of methods, effort may therefore need to be spent optimizing the approximate MM Hamiltonian so that it is a better match for the desired QM/MM Hamiltonian. Alternatively, Iftimie *et al.*²³ show how the replica exchange method^{32,33} (also known as parallel or simulated tempering^{23,34,35}) can be used by adding an additional degree of freedom to the system that enhances sampling.

II. METHODOLOGY AND RESULTS

We here combine the Metropolis-Hastings and Warshel cycle methods together to form an efficient and in principle exact QM/MM free energy method. Using the Warshel free energy cycle (see Fig. 1) the difference in free energy between two systems, A and B, can be estimated using a pure MM Hamiltonian. This estimated free energy can then be corrected by calculating correction free energies that quantify the difference between the QM/MM and MM Hamiltonians for A and B. Rather than estimating these correction free energies using a single-step FEP perturbation, we instead propose to use the Metropolis-Hastings algorithm, as described as part of the MMBIF method (see Fig. 2). We will calculate the correction free energies using the Hamiltonian,

$$H = (1 - \lambda)H_{\text{QM/MM}} + \lambda H_{\text{MM}}. \quad (1)$$

Simulations are then run at different values of λ , and the correction free energy calculated using thermodynamic integration (TI),^{36–38}

$$\begin{aligned} \Delta G_{\text{QM/MM} \rightarrow \text{MM}} &= \int_0^1 \left\langle \frac{\delta G}{\delta \lambda} \right\rangle_{\lambda} d\lambda \\ &= \int_0^1 \left\langle \frac{\delta H}{\delta \lambda} \right\rangle_{\lambda} d\lambda \\ &= \int_0^1 \langle H_{\text{MM}} - H_{\text{QM/MM}} \rangle_{\lambda} d\lambda. \end{aligned} \quad (2)$$

The λ coordinate is used to scale the QM/MM Hamiltonian into the MM Hamiltonian. As the MM Hamiltonian is also used as the approximate potential for the Metropolis-Hastings algorithm, so as λ is increased, H becomes closer to H_{MM} . Therefore as λ is increased, the acceptance probability of the Metropolis-Hastings Monte Carlo moves increases. Replica exchange moves applied across the λ coordinate will therefore enhance QM/MM sampling, in the same manner as the simulated tempering moves used by Iftimie *et al.*²³ However, in this case, no additional replica exchange coordinate is required, as λ is provided naturally by TI. The use of replica exchange moves to enhance sampling along the λ

coordinate provided by TI was first described in the replica exchange thermodynamic integration (RETI) free energy method.³⁹ The RETI method has since been shown to enhance sampling and reduce statistical error in MM free energy calculations,^{30,39–42} and is expected to bring the same advantages to the calculation of the QM/MM correction free energies.

A. The test system

The combined QM/MM free energy method was tested by calculating the relative hydration free energy of water and methane. This calculation is surprisingly complicated because water in water has a completely different solvent structure to methane in water. Thus the calculation involves large reorganization of the solvent, as the dipolar, hydrophilic water molecule is perturbed into the neutral, hydrophobic methane molecule. A large solvent box was used (1679 waters), with periodic boundary conditions, a 15 Å molecule-based electrostatic and nonbonded cutoff, and quadratic smoothing of the intermolecular interactions to zero applied over the last 0.5 Å.⁴³

Two Hamiltonians were required to represent this system; an approximate MM Hamiltonian and the target QM/MM Hamiltonian. In the QM/MM Hamiltonian, the solute was represented using QM, while the surrounding solvent was represented using MM. The QM solute was modeled using MP2/aug-cc-pVDZ, so including the effects of electron correlation. Three different MM water models were investigated; TIP3P,^{44,45} TIP4P,^{44,45} and TIP5P.^{45,46} The electrostatic interaction between the QM and MM regions was modeled using the established method^{1,2,47} of including, within the QM Hamiltonian, the MM point charges. The electrostatic cutoff was applied by including only point charges from atoms that were in solvent molecules within 15 Å of any QM atom (including periodic boundaries). Quadratic smoothing of the electrostatic interactions⁴³ was applied by scaling down the point charges of affected atoms using the smoothing function applied over the last 0.5 Å. The van der Waals interaction between the QM and MM regions was modeled using the Lennard-Jones potential, which was also subject to the same 15 Å molecule-based cutoff with 0.5 Å smoothing function. In the MM Hamiltonian, the QM solute was approximated by a MM solute. For simulations of water in water, the QM water was approximated using the same MM water model as the solvent (i.e., TIP3P, TIP4P, or TIP5P). For simulations of methane in water, the approximation of QM methane was investigated using two MM models; optimized potential for liquid simulations (OPLS) all-atom methane⁴³ and OPLS united-atom methane.⁴⁸

All Monte Carlo simulations were run in the *NPT* ensemble, at 298.15 K, and 1 atm pressure. Preferential sampling^{49,50} was used to enhance sampling around the solute, using a preferential sampling constant of 200 Å. Monte Carlo moves were chosen at random using relative weights of 1600 for solvent moves, 100 for solute moves, and 1 for the volume move. Solute and solvent moves consisted of random, rigid-body translations and rotations, with a 0.2 Å maximum translation and 5° maximum rotation for the sol-

TABLE I. The percentage of Metropolis-Hastings moves accepted during the QM/MM MC simulations.

System	Percentage of accepted moves (%)
Water in TIP3P	50
Water in TIP4P	68
Water in TIP5P	<5 ^a
Methane in TIP3P	90
Methane in TIP4P	90

^aThis simulation was terminated early due to the poor acceptance ratio of the move.

vent molecules, and a 0.1 Å maximum translation and 2.5° maximum rotation for the solute. The volume moves changed the volume of the solvent box by a maximum of 167.9 Å³. As the QM solutes were kept rigid, the gas-phase QM energy of the solute was subtracted from the QM/MM energy, thereby removing the QM intramolecular energy of the solute from the calculation.

B. QM/MM Monte Carlo

We first investigated the efficiency of the Metropolis-Hastings Monte Carlo algorithm by using it to generate long QM/MM trajectories of the test system. We ran QM/MM Monte Carlo simulations of QM water in TIP3P, TIP4P, and TIP5P, and QM methane in TIP3P and TIP4P. The simulations were run in a custom Monte Carlo program,⁵¹ which used MOLPRO⁵² to perform the QM energy calculations.

Based on prior investigation, we found that we could comfortably run the Metropolis-Hastings algorithm using 500 MC moves of the entire system using the approximate MM potential between each QM/MM energy evaluation. This high ratio allowed 50×10^6 steps of MC sampling, requiring just 100 000 QM/MM evaluations, to be performed on each system. The first 10×10^6 steps from each simulation were discarded as equilibration, while averages were calculated over the QM/MM configurations generated over only the last 40×10^6 steps. The approximate MM Hamiltonian used the same MM water model as the solvent to approximate QM water, while the OPLS all-atom methane model was used to approximate QM methane.

The average acceptance ratio of the Metropolis-Hastings moves for each simulation is shown in Table I. While the ratios for water in TIP3P and TIP4P were acceptable, simulations in TIP5P failed to run well. The low acceptance ratio in this case led to the simulation locking up periodically in particular configurations. To investigate this, the structure of the QM water interacting with its nearest neighbor TIP5P water was taken from one of the locked configurations. The interaction energy of the QM water with the MM water was then calculated as a function of intermolecular O–H distance, as the MM water was translated along the intermolecular O–H hydrogen bond vector. The interaction energies are compared in Fig. 3 to those calculated for two QM waters (QM-QM), two TIP5P waters (TIP5P-TIP5P), QM water with TIP3P (TIP3P-QM), and two TIP3P waters (TIP3P-TIP3P). This shows that while the TIP3P-TIP3P and TIP3P-QM potentials agree well, there is very poor agreement between TIP5P-TIP5P and TIP5P-QM. This is despite

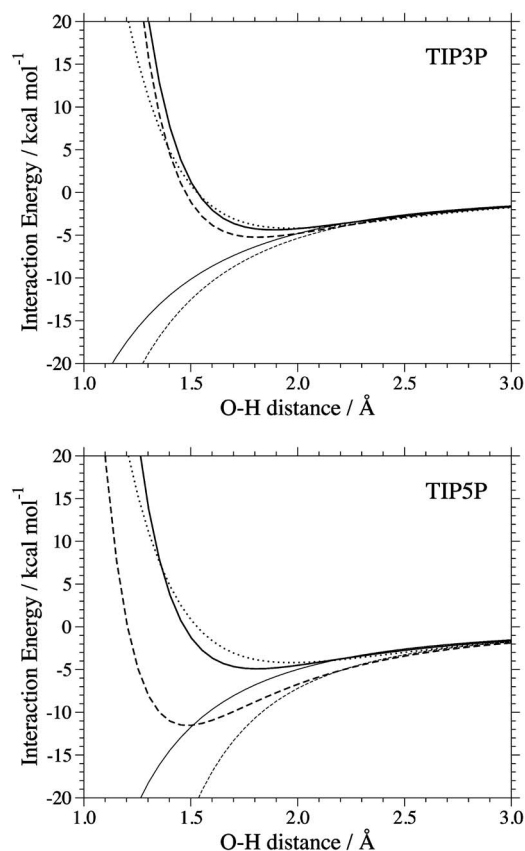


FIG. 3. Interaction energy of a pair of waters as a function of intermolecular O-H distance. The interaction energies of a pair of QM waters (dotted line), a pair of MM waters (bold solid line), and a QM water interacting with a MM water (bold dashed line) are shown. In addition, the electrostatic interaction energy between the pair of MM waters (solid line) and QM and MM waters (dashed line) is also shown. The top figure shows the results for the TIP3P MM water model, while the bottom figure shows the results for the TIP5P MM water model.

TIP3P-TIP3P and TIP5P-TIP5P both being close to QM-QM. The reason for this is seen clearly in the electrostatic interaction energies, also plotted in Fig. 3. These show that the TIP5P-QM electrostatic interaction is significantly more attractive than TIP5P-TIP5P. Examination of the structure at the minimum of TIP5P-QM shows that one of the partial charges representing an oxygen lone pair is embedded within the van der Waals radius of one of the hydrogens of the QM water. This is not physical and is an artifact of the model. Because of this, we believe that, while TIP5P is an excellent water model for MM simulation, it is not suitable for QM/MM simulations, as its use can lead to nonphysical geometries.

The radial distribution functions (RDFs) around the QM water calculated over each of the QM/MM configurations generated over the last 40×10^6 steps of the TIP3P and TIP4P solvent simulations are shown in Fig. 4, while those for QM methane are shown in Fig. 5. The RDFs show key features that agree with other simulation studies^{45,53,54} and with experiments.^{45,54-56} This is highly encouraging, as it is the differences in solute-solvent electrostatics that dominate the difference in solvent structure between water and methane, and all of the solute-solvent electrostatic interactions were calculated using quantum mechanics.

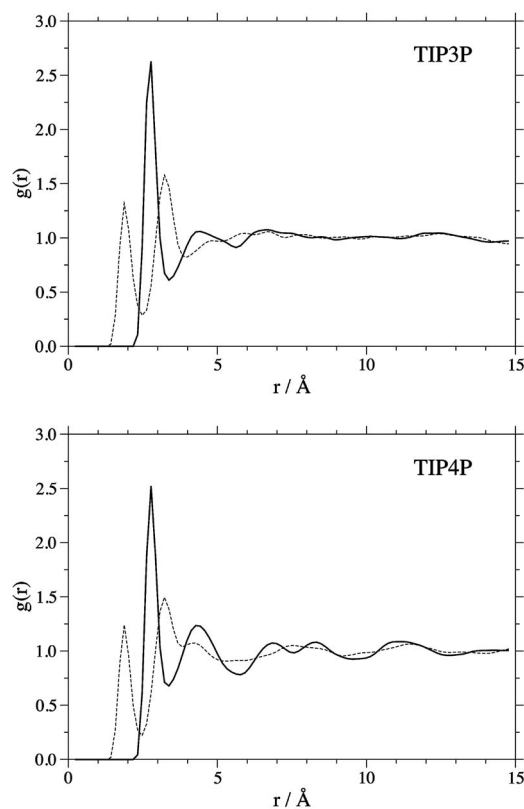


FIG. 4. The oxygen-oxygen (solid line) and oxygen-hydrogen (dashed line) radial distribution functions around the oxygen atom of the QM water, for both TIP3P solvent and TIP4P solvent.

C. QM/MM free energy calculations

The QM/MM Monte Carlo algorithm is now used to generate the QM/MM correction free energies required by the Warshel cycle in Fig. 1. To calculate the correction free energies, RETI simulations were performed using six values of λ , evenly spaced from 0 to 1. Gradients were calculated according to Eq. (2), and these were used to calculate the free energies via TI. Because no atoms were created or deleted, and because Monte Carlo was used, there were no problems with end-point errors that can cause difficulty during molecular dynamics TI calculations.⁵⁷ RETI moves were attempted every 50 000 MC moves. The choice to swap even or odd pairs of replicas was made randomly at each RETI

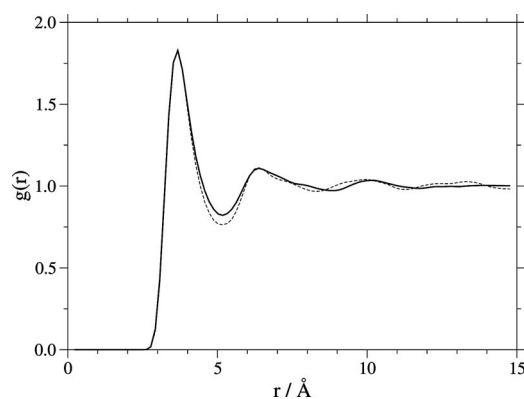


FIG. 5. The carbon-oxygen radial distribution functions around QM methane, for both TIP3P solvent (solid line) and TIP4P solvent (dashed line).

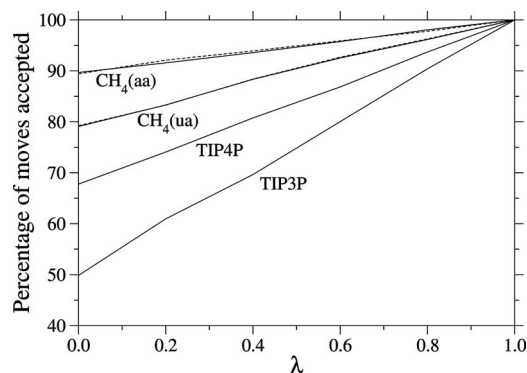


FIG. 6. The percentage of accepted Metropolis-Hastings Monte Carlo moves as a function of λ from each of the QM/MM correction free energy calculations; QM water to TIP3P, QM water to TIP4P, QM water to united-atom methane (in TIP3P: solid line; in TIP4P: dashed line), and QM water to all-atom methane (in TIP3P: solid line; in TIP4P: dashed line).

move.³⁹ The Metropolis-Hastings algorithm was used as before, with each QM/MM energy evaluation separated by 500 MM Monte Carlo moves. 10×10^6 Monte Carlo steps were made for each λ window. Owing to the ratio of one QM/MM energy for every 500 MM moves, only 20 000 QM/MM energy calculations were required for each λ window. All of the correction free energies were calculated using a custom QM/MM Monte Carlo program,⁵¹ with MOLPRO (Ref. 52) used to calculate the QM energies. Correction free energies were calculated to perturb QM water into TIP3P in TIP3P solvent, QM water into TIP4P in TIP4P solvent, and QM methane to OPLS all-atom methane and QM methane to OPLS united-atom methane in both TIP3P and TIP4P solvents.

The Warshel cycle also requires the calculation of the relative hydration free energy of water and methane, as estimated by the MM Hamiltonian. The MM relative hydration free energies were calculated using RETI, over 21 λ windows spaced evenly across a λ coordinate that used to perturb water into methane. All of the simulations were performed using PROTOMS 2.1,^{30,41,42,58} using the same protocols that were used for the QM/MM simulations. RETI moves were attempted every 50 000 steps, and 10×10^6 MC moves were run at each λ window. Relative MM hydration free energies were calculated for all combinations of TIP3P and TIP4P to OPLS all-atom and united-atom methane. The single-topology⁵⁹ perturbation of water into all-atom methane involved the creation of hydrogen atoms, while the perturbation into united-atom methane involved the deletion of hydrogen atoms. To avoid end-point errors in the TI calculation,⁵⁷ constraints were used to ensure that hydrogen atoms that were about to be created or deleted were pulled within the van der Waals sphere of the oxygen/carbon atom as the perturbation progressed.^{39,59} Because these constraints were used, it was not possible to differentiate the MM Hamiltonian analytically with respect to λ . Finite difference thermodynamic integration^{39,60–64} was therefore necessary, which uses the Zwanzig equation,⁶⁵ to calculate numerical free energy gradients, $\Delta G/\Delta\lambda$. A value of $\Delta\lambda=0.001$ was used, with the quality of the numerical gradients verified by using double-wide sampling⁶⁶ to calculate both the forward

TABLE II. The percentage of RETI moves accepted during the QM/MM correction free energy simulations.

Perturbation	Solvent	Percentage of accepted moves (%)
TIP3P \rightarrow QM	TIP3P	76
CH ₄ (ua) \rightarrow QM	TIP3P	88
CH ₄ (aa) \rightarrow QM	TIP3P	93
TIP4P \rightarrow QM	TIP4P	88
CH ₄ (ua) \rightarrow QM	TIP4P	90
CH ₄ (aa) \rightarrow QM	TIP4P	93

($\lambda + \Delta\lambda$) and backward ($\lambda - \Delta\lambda$) values. The backward and forward gradients were found to be equal, within error, for all of the MM simulations performed.

D. Results

The percentage of accepted Metropolis-Hastings Monte Carlo moves as a function of λ for each of the QM/MM correction free energy calculations is shown in Fig. 6. The expected linear relationship is exactly what is observed, with 100% acceptance for $\lambda=1$, when $H=H_{\text{MM}}$. This indicates that λ is an ideal coordinate for replica exchange moves and this is supported by the high acceptance ratio of RETI moves for the QM/MM simulations, shown in Table II. The benefit of using such a good replica exchange coordinate is that all of the replicas are free to move over the entire λ coordinate. This is shown in Fig. 7, which shows the λ trajectory of two replicas from the TIP3P simulation. These two replicas started initially at opposite ends of the λ coordinate, but even with TIP3P having the lowest percentage of accepted RETI moves, both replicas were able to travel across the entire λ coordinate several times during the course of the simulation. This results in improved sampling, the effects of which can be seen in the calculated correction free energies shown in Table III. The correction free energies were calculated over blocks of 50 000 steps. The predicted free energies from each block, for all simulations, were seen to have equilibrated within the first 3.75×10^6 MC steps, so the free energies

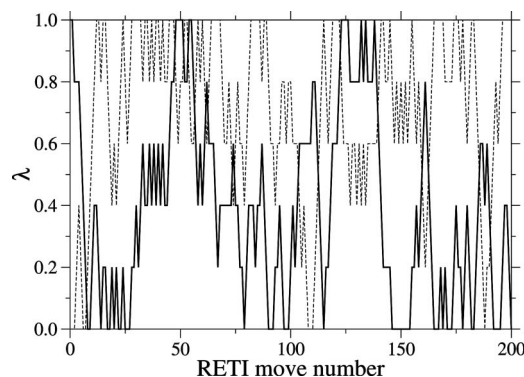


FIG. 7. The λ trajectory for the $\lambda=0$ (dashed line) and $\lambda=1$ (solid line) replicas used to calculate the correction free energy for QM water to TIP3P. While the replicas start at opposite ends of λ , they are both free to explore the entire λ coordinate over the course of the 200 RETI moves that make up the simulation.

TABLE III. The calculated QM/MM correction free energies. The standard error of the average, at the 95% confidence level, is given in parenthesis.

Perturbation	Solvent	ΔG (kcal mol ⁻¹)
TIP3P → QM	TIP3P	-2.15 (0.07)
CH ₄ (ua) → QM	TIP3P	-0.44 (0.02)
CH ₄ (aa) → QM	TIP3P	-0.33 (0.01)
TIP4P → QM	TIP4P	-1.38 (0.03)
CH ₄ (ua) → QM	TIP4P	-0.45 (0.02)
CH ₄ (aa) → QM	TIP4P	-0.28 (0.01)

were calculated over the blocks representing the final 6.25×10^6 steps. The low standard errors indicate the tight convergence of the free energy calculations.

The correction free energy as a function of λ forms a potential of mean force (PMF). None of the PMFs for any of the systems studied were linear. This means that estimates of the free energy based on the gradient evaluated at only a single λ value, e.g., using the QM/MM Hamiltonian at $\lambda = 0$ or using the MM Hamiltonian at $\lambda = 1$, would not be accurate. The perturbation of QM water to TIP3P in TIP3P had the most nonlinear PMF, and is shown, with its gradient, in Fig. 8. The PMF and gradient for TIP4P are also shown for comparison. It is worth noting that while the gradients of the PMF for TIP3P and TIP4P are nearly the same at $\lambda = 1$, where the pure MM Hamiltonian was used to sample phase space, the gradients diverge markedly as λ is decreased. Indeed, by $\lambda = 0$, where the pure QM/MM Hamiltonian was used to sample phase space, the free energy gradients differ by nearly 2 kcal mol⁻¹.

The source of this difference can be seen by looking at the RDFs around the QM water as it is perturbed into TIP3P or TIP4P (Fig. 9). These RDFs reveal a distinct second solvation shell at 4–5 Å around QM water in both TIP3P and TIP4P. However, while this second solvation shell is present in the MM ensemble at $\lambda = 1$ for TIP4P, there is no such feature at $\lambda = 1$ for TIP3P. TIP3P is known to not correctly model the second solvation shell of water.⁴⁵ The free energy difference from QM water to TIP3P in TIP3P solvent must therefore contain both the change in interaction energy to go

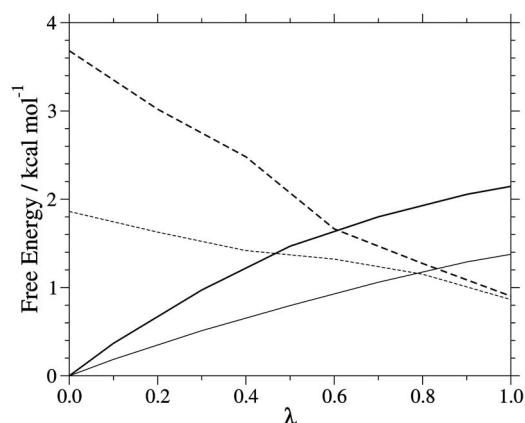


FIG. 8. The potential of mean force (PMF) for the perturbation of QM water into MM water (solid line), together with the gradient of the PMF (dashed line). PMFs and gradients for both TIP3P (bold lines) and TIP4P (faint lines) are shown.

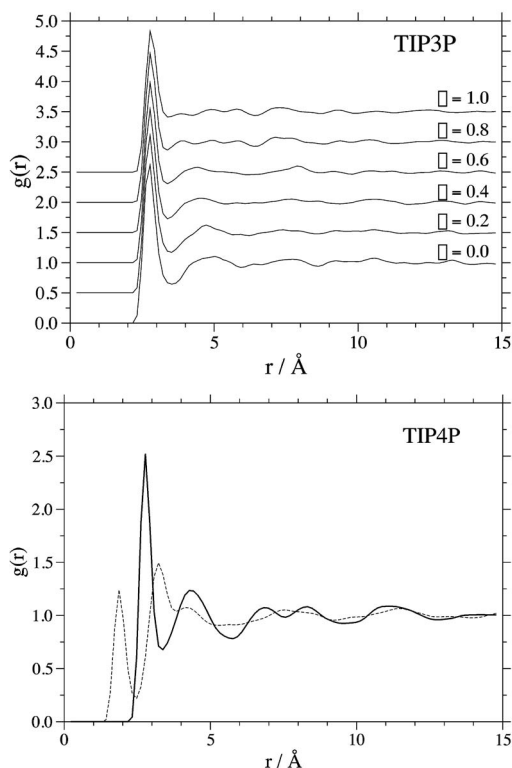


FIG. 9. The oxygen-oxygen radial distribution functions for QM water in MM water, as a function of λ . λ scales the QM water at $\lambda = 0$ into a MM water at $\lambda = 1$. The top figure shows the RDFs for QM water being scaled into TIP3P, in a box of TIP3P, while the bottom figure shows QM water being scaled into TIP4P, in a box of TIP4P.

from QM to TIP3P, and the additional change in entropy necessary to form the second solvation shell. It is this additional change that, we believe, is the source of the difference between the PMFs of TIP3P and TIP4P.

In addition to QM/MM correction free energies, use of the Warshel cycle requires the calculation of the estimated MM relative hydration free energies. These are shown in Table IV. A block analysis showed that these free energies had all equilibrated within the first 3.75×10^6 steps, so averages were collected over the last 6.25×10^6 steps. Standard errors at the 95% confidence level were calculated for these averages, with a low error indicating tight convergence of the free energy calculations. The quality of the calculations was further investigated by calculating the relative free energy

TABLE IV. The calculated MM relative free energies. The standard error of the average, at the 95% confidence level, is given in parenthesis.

Perturbation	Solvent	ΔG (kcal mol ⁻¹)
TIP3P → CH ₄ (ua)	TIP3P	8.8 (0.1)
TIP3P → CH ₄ (aa)	TIP3P	8.9 (0.1)
CH ₄ (ua) → CH ₄ (aa)	TIP3P	0.02 (0.04)
TIP4P → CH ₄ (ua)	TIP4P	8.8 (0.1)
TIP4P → CH ₄ (aa)	TIP4P	8.9 (0.1)
CH ₄ (ua) → CH ₄ (aa)	TIP4P	0.1 (0.05)
TIP3P → TIP4P	TIP3P	0.13 (0.02)
TIP3P → TIP4P	TIP4P	0.05 (0.02)

TABLE V. Calculated QM/MM relative hydration free energies of water and methane. The errors, shown in parenthesis, are based on the combination of the standard errors for the individual components of the calculation.

Solvent	Methane model	ΔG (kcal mol ⁻¹)
TIP3P	CH ₄ (ua)	10.5 (0.1)
TIP3P	CH ₄ (aa)	10.7 (0.1)
TIP4P	CH ₄ (ua)	10.7 (0.1)
TIP4P	CH ₄ (aa)	9.9 (0.1)

needed to perturb united-atom methane into all-atom methane, and TIP3P into TIP4P. The results of these calculations, also shown in Table IV, demonstrate that the closure of the free energy cycle (water → CH₄(ua) → CH₄(aa) → water) is within error for the calculation.

The total QM/MM relative hydration free energy of water and methane, obtained using the Warshel cycle, is shown in Table V.

III. DISCUSSION

The combined Warshel-MMBIF-RETI QM/MM free energy method has been demonstrated to perform extremely well for the calculation of the relative hydration free energy of water and methane. The method captured the change in free energy caused by differences in solvent structure around the QM solvent, and was able to calculate highly converged QM/MM relative free energies efficiently. The three legs of the calculation (the QM/MM free energy corrections at the end points and the estimate of the MM relative free energy) are independent, and can all be run in parallel. QM calculations are only required for the QM/MM correction free energies, and, while several QM/MM simulations are needed across the λ coordinate, these too may be run in parallel. As each λ window required only 20 000 QM/MM evaluations, then the maximum efficiency of the total calculation is determined by the time taken to perform 20 000 QM/MM evaluations (approximately 40 h for MP2/aug-cc-pVDZ water, and 50 h for MP2/aug-cc-pVDZ methane, on a Pentium D 3.2 GHz desktop processor). While the size of the QM region studied in this paper was small, we anticipate that 20 000 evaluations of a large biological system with a ligand-sized QM region are tractable using density functional theory.

While the method has worked well, the calculated QM/MM relative hydration free energies of water and methane, shown in Table V, are at least 1.5 kcal mol⁻¹ greater than the experimental value of 8.31 kcal mol⁻¹.^{39,67} Indeed, the approximate MM relative hydration free energies (8.8 and 8.9 kcal mol⁻¹) are closer to experiment, and the effect of the QM/MM corrections is to reduce the accuracy of the result. The reason for this discrepancy is that the free energies calculated are those of QM water to QM methane in a box of MM solvent. The free energies we have calculated are accurate for this model, but this model gives free energies that are not accurate compared to experiment. This is highlighted by the QM water correction free energies. The free energies necessary to perturb QM water to TIP3P or TIP4P

are both large (>1 kcal mol⁻¹) and almost entirely account for the deviation of the calculated results from experiment. However, these correction free energies represent the perturbation of water into water, in a box of water. Ideally then, the value of these corrections should be zero. The fact that these free energies are not zero is worth noting, as this suggests that, while MM water models perform extremely well in MM simulations, work may be needed to optimize MM water models for QM/MM simulations. It is useful to note that a previous calculation of the relative QM/MM solvation free energy of water and methane also overestimated the free energy⁶⁸ (predicting a relative free energy of 9.6 kcal mol⁻¹). However, in this case, the correction free energy for water was much smaller (0.5 kcal mol⁻¹) than that observed for TIP3P (2.1 kcal mol⁻¹) or TIP4P (1.4 kcal mol⁻¹). This difference could either be caused by the different water model used, different level of QM treatment (density functional theory) or by the use by the previous study of a single-step FEP perturbation to estimate the correction free energies. (Figure 8 shows that were a single-step perturbation at $\lambda = 1$ used in this study, the correction free energies for TIP3P and TIP4P would have both been approximately equal to 0.9 kcal mol⁻¹).

IV. CONCLUSION

By combining existing methodology, we have demonstrated that it is possible to calculate relative QM/MM free energies both efficiently and accurately. The combined method allows consistent, high-quality sampling of complex solvent configurational change, both when perturbing a hydrophilic solute into a hydrophobic solute, and also when moving from a MM Hamiltonian to a QM/MM Hamiltonian. The method has been shown to be efficient, taking around two days to calculate highly converged relative free energies at the MP2/aug-cc-pVDZ/OPLS level, using commodity processors. This method will allow the calculation of QM/MM relative free energies for biological systems. This would allow QM/MM free energies to be calculated for protein-ligand binding and computational enzymology. This is an exciting prospect, with the potential to lead to enhanced accuracy and improved physical descriptors.

ACKNOWLEDGMENTS

We thank the EPSRC, for funding this work (EP/E022197/1), the Centre for Computational Chemistry at the University of Bristol for providing computer resources, and Professor J. W. Essex, Dr. J. Michel and Dr. F. Beierlein for useful discussions. F.R.M. is grateful to the Royal Society for funding.

¹A. Warshel and M. Levitt, *J. Mol. Biol.* **103**, 227 (1976).

²A. Warshel, *Annu. Rev. Biophys. Biomol. Struct.* **32**, 425 (2003).

³M. Garcia-Viloca, J. Gao, M. Karplus, and D. G. Truhlar, *Science* **303**, 186 (2004).

⁴R. A. Friesner and V. Guallar, *Annu. Rev. Phys. Chem.* **56**, 389 (2005).

⁵A. J. Mulholland, *Drug Discovery Today* **10**, 1393 (2005).

⁶F. Claeysens, J. N. Harvey, F. R. Manby, R. A. Mata, A. J. Mulholland, K. E. Ranaghan, M. Schutz, S. Thiel, W. Thiel, and H. J. Werner, *Angew. Chem., Int. Ed.* **45**, 6856 (2006).

⁷L. Masgrau, A. Roujeinikova, L. O. Johannissen, P. Hothi, J. Basran, K.

- E. Ranaghan, A. J. Mulholland, M. J. Sutcliffe, N. S. Scrutton, and D. Leys, *Science* **312**, 237 (2006).
- ⁸F. Beierlein, H. Lanig, G. Schurer, A. H. C. Horn, and T. Clark, *Mol. Phys.* **101**, 2469 (2003).
- ⁹A. E. Cho, V. Guallar, B. J. Berne, and R. Friesner, *J. Comput. Chem.* **26**, 915 (2005).
- ¹⁰A. Khandelwal and S. Balaz, *J. Comput.-Aided Mol. Des.* **21**, 131 (2007).
- ¹¹F. Gräter, S. M. Schwarzl, A. Dejaegere, S. Fischer, and J. C. Smith, *J. Phys. Chem. B* **109**, 10474 (2005).
- ¹²A. Alex and P. Finn, *J. Mol. Struct.: THEOCHEM* **398–399**, 551 (1997).
- ¹³Y. Zhang, H. Liu, and W. Yang, *J. Chem. Phys.* **112**, 3483 (2000).
- ¹⁴G. A. Cisneros, H. Liu, Y. Zhang, and W. Yang, *J. Am. Chem. Soc.* **125**, 10384 (2003).
- ¹⁵G. A. Kaminski and W. L. Jorgensen, *J. Phys. Chem. B* **102**, 1787 (1998).
- ¹⁶O. Acevedo, W. L. Jorgensen, and J. D. Evanseck, *J. Chem. Theory Comput.* **3**, 132 (2007).
- ¹⁷R. P. Muller and A. Warshel, *J. Phys. Chem.* **99**, 17516 (1995).
- ¹⁸M. Štrajbl, G. Hong, and A. Warshel, *J. Phys. Chem.* **106**, 13333 (2002).
- ¹⁹R. H. Wood, E. M. Yezdimer, S. Sakane, J. A. Barriocanal, and D. J. Doren, *J. Chem. Phys.* **110**, 1329 (1999).
- ²⁰Y. Ming, G. Lai, C. Tong, R. H. Wood, and D. J. Doren, *J. Chem. Phys.* **121**, 773 (2004).
- ²¹T. H. Rod and U. Ryde, *J. Chem. Theory Comput.* **1**, 1240 (2005).
- ²²R. Iftimie, D. Salahub, and D. Wei, *J. Chem. Phys.* **113**, 4852 (2000).
- ²³R. Iftimie, D. Salahub, and J. Schofield, *J. Chem. Phys.* **119**, 11285 (2003).
- ²⁴P. Bandyopadhyay, *J. Chem. Phys.* **122**, 091102 (2005).
- ²⁵M. H. M. Olsson, G. Hong, and A. Warshel, *J. Am. Chem. Soc.* **125**, 5025 (2003).
- ²⁶E. Rosta, M. Klähn, and A. Warshel, *J. Phys. Chem. B* **110**, 2934 (2006).
- ²⁷W. K. Hastings, *Biometrika* **57**, 97 (1970).
- ²⁸B. Hetényi, K. Bernacki, and B. J. Berne, *J. Chem. Phys.* **117**, 8203 (2002).
- ²⁹L. D. Gelb, *J. Chem. Phys.* **118**, 7748 (2003).
- ³⁰J. Michel, R. D. Taylor, and J. W. Essex, *J. Chem. Theory Comput.* **2**, 732 (2006).
- ³¹K. Bernacki, B. Hetényi, and B. J. Berne, *J. Chem. Phys.* **121**, 44 (2004).
- ³²Y. Sugita, A. Kitao, and Y. Okamoto, *J. Chem. Phys.* **113**, 6042 (2000).
- ³³H. Fukunishi, O. Watanabe, and S. Takada, *J. Chem. Phys.* **116**, 9058 (2002).
- ³⁴U. H. E. Hansmann, *Chem. Phys. Lett.* **281**, 140 (1997).
- ³⁵Y. Sugita and Y. Okamoto, *Chem. Phys. Lett.* **314**, 141 (1999).
- ³⁶X. Barril, M. Orozco, and F. J. Luque, *J. Med. Chem.* **42**, 5110 (1999).
- ³⁷B. C. Oostenbrink, J. W. Pitera, M. M. H. Lipzig, J. H. N. Meerman, and W. F. V. Gunsteren, *J. Med. Chem.* **43**, 4596 (2000).
- ³⁸D. A. Pearlman and P. S. Charifson, *J. Med. Chem.* **44**, 3417 (2001).
- ³⁹C. J. Woods, M. A. King, and J. W. Essex, *J. Phys. Chem. B* **107**, 13703 (2003).
- ⁴⁰C. J. Woods, M. A. King, and J. W. Essex, *J. Phys. Chem. B* **107**, 13711 (2003).
- ⁴¹J. Michel, M. L. Verdonk, and J. W. Essex, *J. Med. Chem.* **49**, 7427 (2006).
- ⁴²C. Barillari, J. Taylor, R. Viner, and J. W. Essex, *J. Am. Chem. Soc.* **129**, 2577 (2007).
- ⁴³W. L. Jorgensen, D. S. Maxwell, and J. Tirado-Rives, *J. Am. Chem. Soc.* **118**, 11225 (1996).
- ⁴⁴W. L. Jorgensen, J. Chandrasekhar, J. D. Madura, R. W. Impey, and M. L. Klein, *J. Chem. Phys.* **79**, 926 (1983).
- ⁴⁵W. L. Jorgensen and J. Tirado-Rives, *Proc. Natl. Acad. Sci. U.S.A.* **102**, 6665 (2003).
- ⁴⁶M. W. Mahoney and W. L. Jorgensen, *J. Chem. Phys.* **112**, 8910 (2000).
- ⁴⁷J. Gao, *Acc. Chem. Res.* **29**, 298 (1996).
- ⁴⁸W. L. Jorgensen, J. D. Madura, and C. J. Swenson, *J. Am. Chem. Soc.* **106**, 6638 (1984).
- ⁴⁹J. C. Owicki and H. A. Scheraga, *Chem. Phys. Lett.* **47**, 600 (1977).
- ⁵⁰W. L. Jorgensen, *J. Phys. Chem.* **87**, 5304 (1983).
- ⁵¹C. J. Woods, SIRE, a complete molecular simulation framework, in development, see <http://siremol.org>
- ⁵²H. J. Werner, P. J. Knowles, R. Lindh, F. R. Manby, M. Schütz, P. Celani, T. Korona, G. Rauhut, R. D. Amos, A. Bernhardsson *et al.*, MOLPRO, version 2006.2, a package of ab initio programs (2006), see <http://www.molpro.net>
- ⁵³J. Hernández-Cobos, A. D. Mackie, and L. F. Vega, *J. Chem. Phys.* **114**, 7527 (2001).
- ⁵⁴A. K. Soper, *Chem. Phys.* **258**, 121 (2000).
- ⁵⁵P. H. K. D. Jong, J. E. Wilson, G. W. Neilson, and A. D. Buckingham, *Mol. Phys.* **91**, 99 (1997).
- ⁵⁶T. Head-Gordon and G. Hura, *Chem. Rev. (Washington, D.C.)* **102**, 2651 (2002).
- ⁵⁷D. Min, H. Li, G. Li, R. Bitetti-Putzer, and W. Yang, *J. Chem. Phys.* **126**, 144109 (2007).
- ⁵⁸C. J. Woods and J. Michel, PROTOMS 2.1, a Monte Carlo free energy program (2006).
- ⁵⁹D. A. Pearlman, *J. Phys. Chem.* **98**, 1487 (1994).
- ⁶⁰M. Mezei, *J. Chem. Phys.* **86**, 7084 (1987).
- ⁶¹C. R. W. Guimaraes and R. B. Alencastro, *Int. J. Quantum Chem.* **85**, 713 (2001).
- ⁶²C. R. W. Guimaraes and R. B. Alencastro, *J. Med. Chem.* **45**, 4995 (2002).
- ⁶³C. R. W. Guimaraes and R. B. Alencastro, *J. Phys. Chem. B* **106**, 466 (2002).
- ⁶⁴S. Kamath, E. Couthinho, and P. Desai, *J. Biol. Phys.* **16**, 1239 (1999).
- ⁶⁵R. W. Zwanzig, *J. Chem. Phys.* **22**, 1420 (1954).
- ⁶⁶W. L. Jorgensen and C. Ravimohan, *J. Chem. Phys.* **83**, 3050 (1985).
- ⁶⁷T. H. Zhu, J. B. Li, G. D. Hawkins, C. J. Cramer, and D. G. Truhlar, *J. Chem. Phys.* **109**, 9117 (1998).
- ⁶⁸T. Wesolowski and A. Warshel, *J. Phys. Chem.* **98**, 5183 (1994).